Available online at www.sciencedirect.com
SCIENCE DIRECT®
International Journal of Heat and Mass Transfer 48 (2005) 4766–4778
International Journal of HEAT and MASS TRANSFER
www.elsevier.com/locate/ijhmt

Correlations for the mass transfer rate of droplets in vertical upward annular flow

Tomio Okawa *, Isao Kataoka

Department of Mechanophysics Engineering, Osaka University, 2-1, Yamadaoka, Suita-shi, Osaka 565-0871, Japan

Received 13 August 2003; received in revised form 18 May 2005
Available online 19 August 2005

Abstract

New correlations for the deposition rate and entrainment rate of droplets in vertical upward annular flow were developed from simple models and available experimental data. In the correlation for the deposition rate, the superficial gas velocity was used as the parameter of primary importance at low droplet concentration while the droplet concentration itself at high droplet concentration. In correlating the rate of droplet entrainment, the ratio of interfacial shear force to the surface tension force acting on the surface of liquid film was the appropriate scaling parameter to correlate the experimental data measured in varied conditions. The experimental data for air–water annular flow were used in the development of the present correlations since extensive databases were available. It was however confirmed that the present model provides satisfactory agreements with the experimental data for high-pressure steam–water annular flow.

Keywords: Annular flow; Droplet; Deposition; Entrainment; Correlation

1. Introduction

In annular two-phase flow, part of the liquid flows along the wall as a liquid film and part as droplets in the gas core flow. The heat and mass transfer processes in this flow configuration are largely influenced by the fraction of the droplets entrained in the high velocity gas. The entrained fraction of liquid is the consequence of the two rate processes: the droplet deposition on to the liquid film and the droplet entrainment from the liquid film. The accurate correlations for the rates of deposition and entrainment are hence of significant practical importance in various industrial applications, including nuclear power plants, boilers, evaporators and condensers. In particular, it is known that the depletion of liquid film is the fairly good approximation to the onset of critical heat flux condition in flow boiling if the two-phase flow pattern is annular flow. The reliable correlations for the deposition and entrainment rates of droplets are therefore of particular interest to confirm the safety of light water reactors.

The correlations for the deposition rate that were available in literature were reviewed in detail by Matsuura [1]. Alexander and Colden [2], Paleev and Filippovich [3], Yanai [4], Namie and Ueda [5,6], Andreussi [7], Schadel et al. [8] among others carried out the experiments to deduce the correlations for the deposition rate. It was reported that the resulting correlations predicted the experimental data well. However, since

* Corresponding author. Tel.: +81 6 6879 7257; fax: +81 6 6879 7247.
E-mail address: t-okawa@mech.eng.osaka-u.ac.jp (T. Okawa).

0017-9310/$ - see front matter © 2005 Elsevier Ltd. All rights reserved.
doi:10.1016/j.ijheatmasstransfer.2005.06.014

Nomenclature

C	droplet concentration (kg/m^3)
C^*	dimensionless droplet concentration [$= C/\rho_g$]
D	tube diameter (m)
E	entrainment fraction
f_i	interfacial friction factor
f_w	wall friction factor
f_z	correction function for z^*, see Eq. (7)
g	gravitational acceleration (m/s^2)
h_{gl}	latent heat of vaporization (J/kg)
J	volumetric flux (m/s)
k_d	deposition mass transfer coefficient (m/s)
k^*	dimensionless deposition mass transfer coefficient [$= k_d(\rho_g D/\sigma)^{0.5}$]
k_0	dimensionless deposition mass transfer coefficient when z_d approaches zero
k_e	proportionality factor (m/s)
m_d	deposition rate (kg/m^{2}s)
m_e	entrainment rate (kg/m^{2}s)
q_{chf}	local heat flux at the dryout point (W/m^2)
Re	Reynolds number
U_e	volumetric entrainment rate (m/s)
u	velocity (m/s)
u_f	friction velocity (m/s)
z_d	deposition length (m)
z^*	dimensionless deposition length [$= z_d/D$]

Greek symbols

$\Delta\rho$	density difference between gas and liquid phases (kg/m^3)
δ	film thickness (m)
ε_1	mean fractional error
ε_2	standard deviation in fractional error
μ	viscosity (Pa s)
π_e	dimensionless parameter defined by Eq. (15)
π_{e1}	modified π_e to account critical gas velocity
ρ	density (kg/m^3)
σ	surface tension (N/m)

Subscripts

0	influence of deposition length is corrected
c	critical
cal	calculated
d	deposition
e	entrainment
eq	equilibrium
exp	experimental
f	liquid film
g	gas phase
l	liquid phase

these correlations were based primarily on their respective experimental data, validity in wider ranges of thermal hydraulic conditions was not shown clearly. In fact, Matsuura pointed out in some typical conditions for boiling water reactors that the predicted results from these correlations exhibited significant scattering that could be up to more than one order of magnitude [1]. Goldmann et al. [9], Whalley and Hewitt [10], Saito et al. [11], Sugawara [12], Govan et al. [13] and Okawa et al. [14] used available experimental databases to develop the correlations for the deposition rate. These correlations are useful to understand the influences of various parameters such as fluid properties, gas velocity and droplet concentration. In these studies, however, the parameters adopted to correlate the deposition rate were not sufficient to achieve good agreement with the data or the accumulation of experimental data was not very extensive. McCoy and Hanratty [15] compiled the experimental data of deposition rate measured in dilute particle concentrations and found that the deposition mass transfer coefficient is correlated well with the particle relaxation time. This result gave important information on the mechanism of droplet deposition but the requirement for the droplet concentration is not satisfied in many practical applications.

In annular two-phase flow, the droplet entrainment usually coexists with the droplet deposition. Thus, the measurement of entrainment rate is difficult and few results of direct measurement were reported in literature. Consequently, many correlations for the entrainment rate were developed from the experimental data or the available correlations for the droplet flowrate in the hydrodynamic equilibrium state [10–14,16–19], in which the entrainment rate may be balanced with the deposition rate. It should however be kept in mind that the entrainment rate deduced from the droplet flowrate in the equilibrium state includes the error in predicting the deposition rate from an empirical correlation.

The literature review indicated that a number of experimental and theoretical works have been conducted for the droplet transfer in annular two-phase flow but further improvements of the correlations for the deposition and entrainment rates are still required because of their significant importance in many practical applications. The main purpose of this study is to develop the reliable correlations for the deposition and entrainment rates in vertical upward annular two-phase flow. Phenomenological approach is adopted in developing the correlations due to the extreme complexity of these rate processes. Thus, the resultant correlations contain

several empirical constants. To determine these constants, experimental data for air–water upward annular flow in round tubes are used since extensive databases are available. Validity of the present models in wider range of flow condition is tested against the experimental data for high-pressure steam–water annular flow.

2. Correlation for the deposition rate

2.1. General trend of experimental data for air–water annular flow

Measurements of the rate of droplet deposition m_d for vertical upward annular two-phase flow in round tubes were conducted extensively using air and water as test fluids. In order to express m_d with simple equations, it is generally assumed that m_d is proportional to the droplet concentration in the gas core C:

$$m_d = k_d C \tag{1}$$

where k_d is the deposition mass transfer coefficient. The experimental databases that are used to develop the correlation for k_d in this study are listed in Table 1 [8,13,20,21]. In these experiments, the two different methods were used for the measurement of m_d: the film removal and redeposition (double film extraction) method [13,20,21] and the tracer mixing method [8]. The principles of these measurement techniques are found in Hewitt [22]. The range of tube inside diameter is 5.0–57.2 mm in these experimental databases. In the double film extraction method, the liquid film is completely removed at the first liquid film extraction unit but a new liquid film is built up downstream the first unit due to the deposition of remaining droplets. The new liquid film is removed at the second liquid film extraction unit to measure the deposition rate between the first and second units. In Table 1, z_d denotes the deposition length that is the distance between the two units. In the tracer mixing method, the axial variation of tracer concentration within liquid film is measured in the quasi-equilibrium state sufficiently downstream from the gas–liquid mixing section to deduce the mass transfer rate between droplets and liquid film, and consequently z_d is indeterminate. Shown in the last five columns in Table 1 are the number of experimental data used in the model development N, the mean fractional error ε_1 and the standard deviation in the fractional error ε_2 when the correlations proposed later are used to predict the deposition rate and entrainment rate; the subscripts d and e imply the deposition and entrainment, respectively.

Whalley and Hewitt [10] used the surface tension to correlate k_d but most available correlations used the superficial gas velocity J_g and/or the droplet concentration in the gas core C as the parameter of primary importance [2–9,11–14]. It might be interesting to note that many available correlations account the influences of both J_g and C [3,5–7,12] but older correlations do not include C [2,4,9] while several recent correlations do not include J_g [8,11,13,14]. In view of this, the measured values of k_d in the experimental databases listed in Table 1 are plotted against J_g and C in Fig. 1(a) and (b), respectively. It is seen in these figures that the influence of J_g on k_d is rather obscure while k_d decreases monotonously with the increase in C. However, a closer look at Fig. 1(b) reveals that there exists significant scattering of k_d and the dependence of k_d on C is not clear at low droplet concentration. The dependence of k_d on J_g when C is smaller than 0.5 kg/m^3 is shown in Fig. 2. It is found in this low droplet concentration condition that k_d increases with J_g in each experimental database.

2.2. Model development at high droplet concentration

Fig. 1(b) suggests that C is the parameter of primary importance if the droplet concentration in the gas core is sufficiently high. Govan et al. [13] investigated the influence of C on k_d and found that the dimensionless droplet mass transfer coefficients k^* measured for various fluids are correlated well with the dimensionless droplet concentration C^*. The definitions of k^* and C^* are given by

$$k^* = k_d \sqrt{\frac{\rho_g D}{\sigma}} \tag{2}$$

$$C^* = \frac{C}{\rho_g} \tag{3}$$

Based on this result, Govan et al. [13] proposed the empirical correlation for k_d; Okawa et al. [14] also

Table 1
Experiments for the deposition rate in vertical upward air–water annular flow

References	Measurement technique	D (mm)	z_d/D	N	ε_{1d}	ε_{2d}	ε_{1e}	ε_{2e}
Cousins and Hewitt [20]	Double film extraction	9.5	16–192	131	−0.14	0.19	0.09	0.20
Cousins and Hewitt [20]	Double film extraction	31.8	11–61	17	−0.13	0.19	−0.07	0.25
Govan et al. [13]	Double film extraction	31.8	14	34	−0.04	0.15	−0.06	0.24
Schadel et al. [8]	Tracer method	25.4	–	24	−0.08	0.21	–	–
Schadel et al. [8]	Tracer method	42.0	–	20	−0.09	0.20	–	–
Schadel et al. [8]	Tracer method	57.2	–	14	0.04	0.22	–	–
Okawa et al. [21]	Double film extraction	5.0	36	34	0.06	0.22	−0.14	0.19

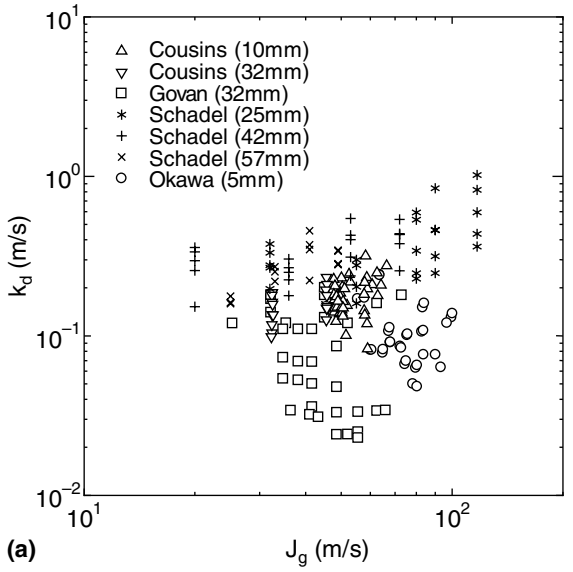

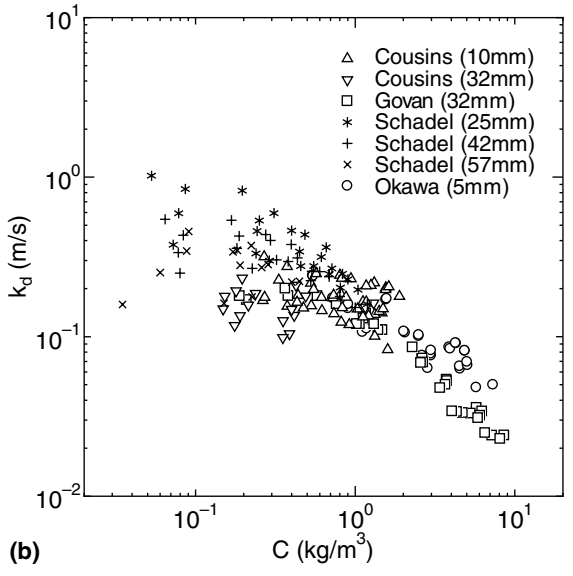

Fig. 1. Deposition mass transfer coefficients measured in air–water annular flow: (a) dependence on superficial gas velocity, (b) dependence on droplet concentration.

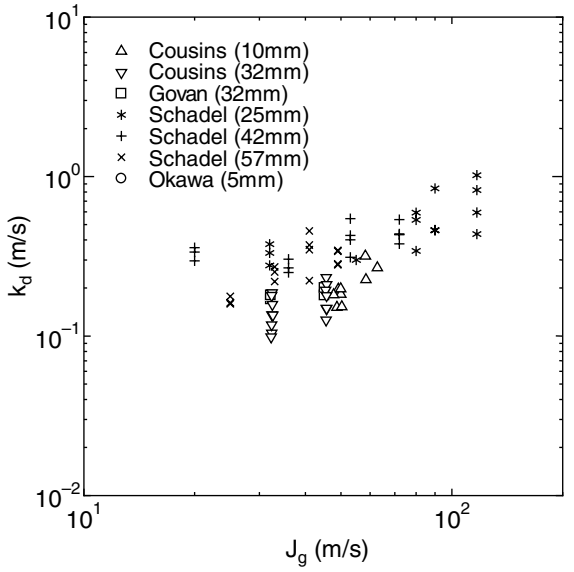

Fig. 2. Dependence of deposition mass transfer coefficient on superficial gas velocity in air–water annular flow at low droplet concentration ($C < 0.5$ kg/m^3).

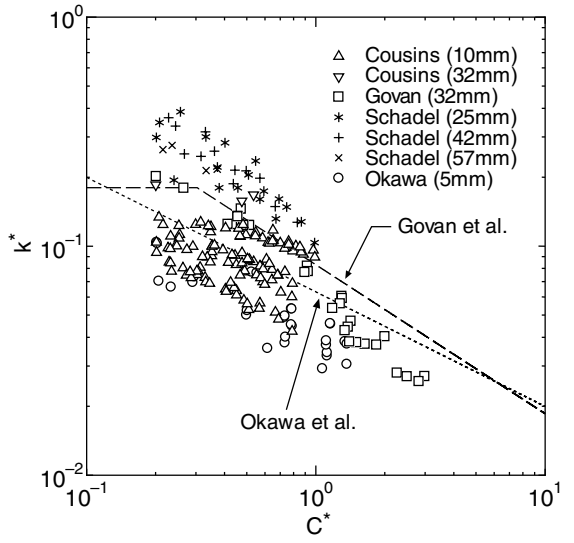

Fig. 3. Dependence of dimensionless deposition mass transfer coefficient on dimensionless droplet concentration ($C^* > 0.2$).

deduced the empirical correlation for k_d from the same experimental data. The values of k^* calculated from the experimental data listed in Table 1 are plotted against C^* in Fig. 3. In the figure, the data are plotted when C^* is greater than 0.2. The dashed line and the dotted line in the figure denote the following correlations by Govan et al. [13] and Okawa et al. [14], respectively:

$$k^* = \min\left\{0.18, 0.083(C^*)^{-0.65}\right\} \quad (4)$$

$$k^* = 0.0632(C^*)^{-0.5} \quad (5)$$

where min $\{A, B\}$ denotes the smaller value of A and B. The above two correlations roughly capture the dependence of k^* on C^* in high droplet concentration condition but there exists significant scattering. In particular, the figure indicates that the two correlations have the tendency to overestimate the data obtained with the double film extraction technique while underestimate those with the tracer method. Cousins and Hewitt

[20] found from their experiments using the double film extraction technique that k_d initially decreases rapidly with the increase in z_d and then approaches to an asymptotic value for long z_d. This would be because the large droplets and/or the droplets having large transverse velocity at their inception at film surface impact the wall within a short distance from the first film extraction unit. To eliminate the dependence of k_d on z_d, Govan et al. selected the experimental data that were obtained using relatively short deposition lengths ($14 < z_d/D < 19$). In the tracer method, the deposition rate is deduced from the tracer concentration within liquid film in the equilibrium state in which the droplet entrainment coexists with the droplet deposition. The deposition length in this method could hence be assumed zero. On the other hand, the deposition lengths adopted in most double film extraction experiments listed in Table 1 are longer than that selected by Govan et al. The difference in the deposition length is hence expected the primary cause of the scattering found in Fig. 3. Furthermore, Fig. 3 indicates that k^* is roughly proportional to $(C^*)^{-0.8}$ if C^* is sufficiently high. Thus, in order to elucidate the dependence of k^* on the dimensionless deposition length $z^* = z_d/D$, the values of $k^*(C^*)^{0.8}$ are plotted against z^* in Fig. 4. The figure confirms that k^* initially decreases with z^* and then approaches to approximately 28% of the initial value for long z^*. The effect of z^* on k^* should be dependent on the distributions of droplet size and the initial droplet velocity in the transverse direction. It is hence considered that the influences of various parameters including tube diameter, droplet concentration, film flowrate and gas phase velocity should be accounted to express the effect of z^* correctly. Nonetheless, Fig. 4 indicates that the following simple expression may be sufficient as the first approximation to account the effect of z^* for the present experimental databases:

$$k^*(C^*)^{0.8} \propto 0.28 + 0.72e^{-0.06z^*} \tag{6}$$

This would be the main reason why k^* is correlated successfully with C^* if a certain range of z^* is used to select the data [13]. In usual situations of annular two-phase flow, the droplet entrainment coexists with the droplet deposition, and consequently z_d equals zero. This implies that z_d should approach zero in the double film extraction experiments in order to measure the correct value of k_d. This procedure is however practically impossible. Hence, the value of k^* when z^* approaches zero, that is denoted by k_0, is estimated through Eq. (6):

$$k_0 = k^* f_z \tag{7}$$

where f_z is the correction function for z^* and is defined by

$$f_z = \frac{1}{0.28 + 0.72e^{-0.06z^*}} \tag{8}$$

Note that f_z equals unity if z_d is zero and f_z approaches an asymptotic value for long z_d. The values of k_0 that are calculated from the experimental data listed in Table 1 are plotted against C^* in Fig. 5. The figure demonstrates that the scattering is markedly reduced if the influence of z^* is corrected. Though there still exists scattering, the following empirical correlation gives a reasonable fit for the air–water data at high droplet concentration:

$$k_0 = \min\left\{0.19(C^*)^{-0.2}, 0.105(C^*)^{-0.8}\right\} \tag{9}$$

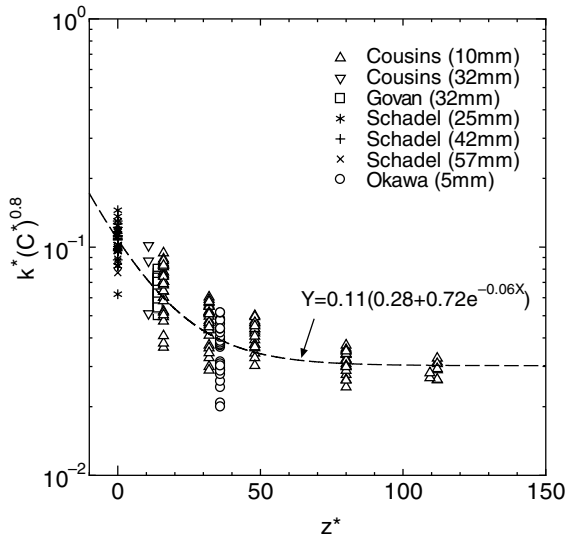

Fig. 4. Effect of deposition length on deposition mass transfer coefficient at high droplet concentration ($C^* > 0.2$).

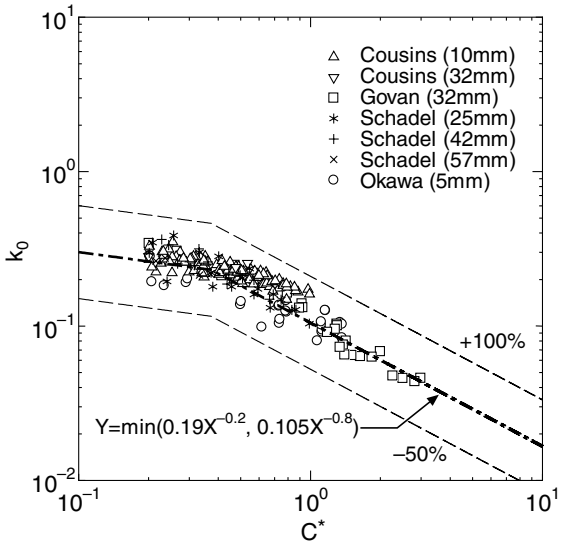

Fig. 5. Proposed correlation for the deposition mass transfer coefficient at high droplet concentration ($C^* > 0.2$).

In annular two-phase flow, there exist droplets of various sizes [23] and the droplets may have various initial transverse velocities at the instant of atomization [24]. Since the effects of these parameters have not been thoroughly understood, the empirical approach was adopted here to correct the influence of z^*. It would hence be required to include the effects of the size distribution of droplets and the droplet initial transverse velocity for the mechanistic modelling.

2.3. Model development at low droplet concentration

Fig. 2 indicates that k_d is roughly proportional to J_g at low droplet concentration in each experimental database. This is consistent with the fact that the dimensionless deposition mass transfer coefficient is defined by k_d/J_g [3–6,9,12] or k_d/u_f [7,15] in existing correlations, where u_f denotes the friction velocity. Thus, the data in which C^* is smaller than 0.15 are plotted against u_f in Fig. 6. Here, in the calculation of u_f, the wall friction factor f_w is evaluated by

$$f_w = 0.0791 Re_g^{-0.25} \tag{10}$$

In Fig. 6, the prediction with the following correlation by McCoy and Hanratty [15] for long particle relaxation time is drawn with the dashed line:

$$k_d = 0.17 u_f \tag{11}$$

It is found that the data obtained with the tracer mixing method by Schadel et al. [8] agree with the above correlation well but the data with the double film extraction method are generally overpredicted. Postulating that the difference in the deposition length is the main cause of this discrepancy, the influence of z^* is investigated in Fig. 7. The figure indicates that the following correction function is appropriate in this low droplet concentration condition:

$$f_z = \frac{1}{0.4 + 0.6e^{-0.05z^*}} \tag{12}$$

This equation implies that k_d decreases to approximately 40% of the initial value for long z^*. The influence of z^* is

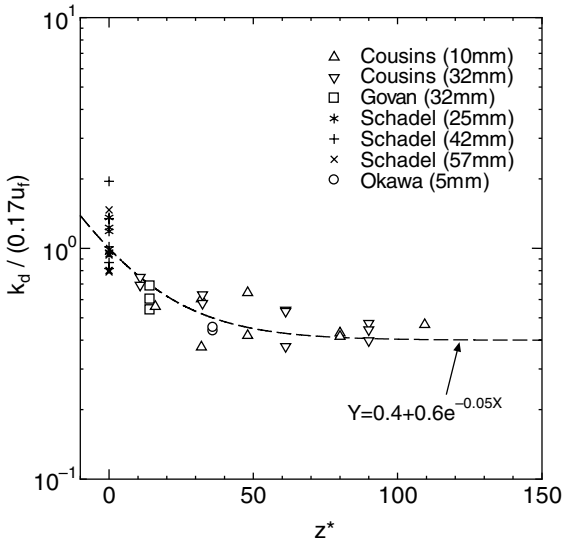

Fig. 7. Effects of deposition length on deposition mass transfer coefficient at low droplet concentration.

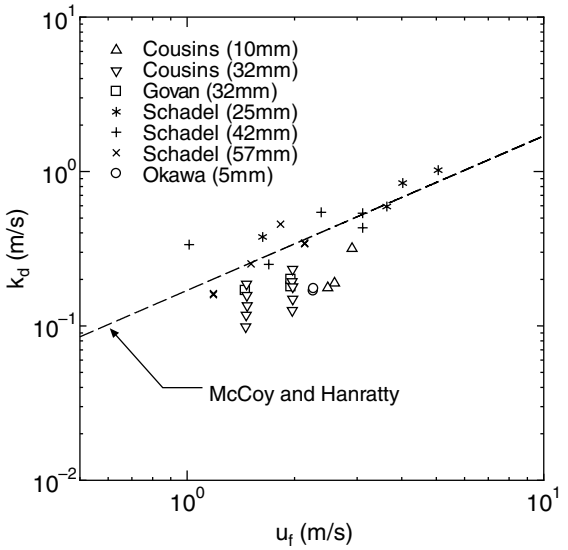

Fig. 6. Dependence of deposition mass transfer coefficient on friction velocity in low droplet concentration experiments.

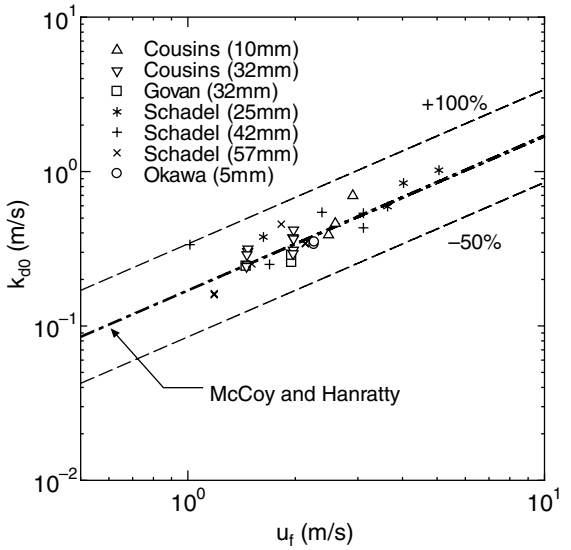

Fig. 8. Proposed correlation for the deposition mass transfer coefficient at low droplet concentration.

hence less significant comparing with the result at high droplet concentration. This may be because the size distribution of droplets is rather uniform at low droplet concentration. The corrected deposition mass transfer coefficients k_{d0} ($k_{d0} = k_d f_z$) are plotted against u_f in Fig. 8. The figure indicates that the experimental data agree well with the correlation by McCoy and Hanratty if the effect of z^* is corrected.

3. Correlation for the entrainment rate

3.1. Experimental databases

Many available correlations for the entrainment rate were developed from the experimental data of entrainment fraction in the quasi-equilibrium state [10–14,16–19]. To deduce the entrainment rate from the equilibrium entrainment fraction, the correlation for the deposition rate is required. Thus, to eliminate the error included in the correlation for the deposition rate, a different approach is adopted here. In the hydrodynamic equilibrium state sufficiently downstream from the gas–liquid mixing section, the entrainment and deposition rates of droplets are considered equal in adiabatic annular two-phase flow. Using this concept, the correlation for the entrainment rate can be developed from the available experimental data of deposition rate measured in quasi-equilibrium state [25]. In this case, an empirical correlation for the deposition rate is not necessary to deduce the entrainment rate from experimental data.

The experimental databases by Govan et al. [13], Cousins and Hewitt [20] and Okawa et al. [21], that were developed originally for the deposition rate, are used in the present model development study for the entrainment rate. If the annular flow does not reach the equilibrium state, the measured deposition rate is not regarded as the entrainment rate. The data are thus eliminated if the distance between the gas–liquid mixing section and the measuring section is shorter than the prediction by the following correlation by Ishii and Mishima [26]:

$$z_{eq} = 600D\sqrt{\frac{J_g}{Re_f}\left\{\frac{\rho_g^2}{\sigma g\Delta\rho}\left(\frac{\Delta\rho}{\rho_g}\right)^{2/3}\right\}^{1/4}} \tag{13}$$

where z_{eq} is the distance necessary to reach an equilibrium condition. In these experimental databases, the droplet transfer rates were measured with the double film extraction method. Thus, the following equation is used to eliminate the influence of deposition length:

$$m_{e0} = m_{d0} = m_{d,exp} f_z \tag{14}$$

where $m_{d,exp}$ denotes the deposition rate measured in the experiment. Note that m_{d0} and $m_{d,exp}$ are equal if z^* is zero. From the investigations for deposition rate, the boundary of C^* for low and high droplet concentrations may be around 0.15. Thus, f_z in Eq. (14) is calculated from Eq. (8) if $C^* > 0.15$ while from Eq. (12) if $C^* < 0.15$.

3.2. Model development

Okawa et al. [14,19] showed that the equilibrium entrainment fractions measured for various fluids are correlated well if the volumetric flowrate of entrained liquid U_e ($U_e = m_e/\rho_l$) is assumed proportional to the dimensionless parameter π_e. The definition of π_e is given by

$$\pi_e = \frac{f_i \rho_g J_g^2}{\sigma/\delta} \tag{15}$$

where f_i is the interfacial friction factor and δ is the film thickness. Here, π_e denotes the ratio of the interfacial shear force to the surface tension force acting on the surface of liquid film. The correlation by Wallis [27] is used to evaluate f_i:

$$f_i = 0.005\left(1 + 300\frac{\delta}{D}\right) \tag{16}$$

The film thickness δ is calculated using the following relation:

$$f_i \rho_g J_g^2 \cong f_w \rho_l \left(\frac{D}{4\delta} J_f\right)^2 \tag{17}$$

To derive Eq. (17), it is assumed that the interfacial shear force and the wall friction force acting on the liquid film are equal ($f_i \rho_g u_g^2 \cong f_w \rho_l u_f^2$) and liquid film is thin ($u_g \cong J_g$; $4u_f\delta \cong J_f D$); also, the wall friction factor f_w is assumed constant ($f_w = 0.005$) for simplicity.

The experimental data of the volumetric entrainment rate $U_{e,exp} = m_{d,exp}/\rho_l$ and of the corrected one $U_{e0} = m_{d0}/\rho_l$ are plotted against π_e in Fig. 9(a) and (b), respectively. It is confirmed that the experimental data of U_e may be expressed as the function of π_e. It is hence considered that π_e is an appropriate scaling parameter to correlate the entrainment rate. The comparison between Fig. 9(a) and (b) reveals that the scattering is less significant for U_{e0}. This may support that the influence of deposition length is corrected fairly well with Eq. (14). Though Okawa et al. [14,19] simply postulated that U_e is proportional to π_e, Fig. 9(b) indicates that the dependence on π_e appears to become less significant with the increase in π_e.

It is experimentally known that J_g should be greater than the critical value J_{gc} for the atomization to occur at the surface of liquid film. To simply account this phenomenon, π_e is modified to π_{e1} as

$$\pi_{e1} = \frac{f_i \rho_g (J_g^2 - J_{gc}^2)}{\sigma/\delta} \tag{18}$$

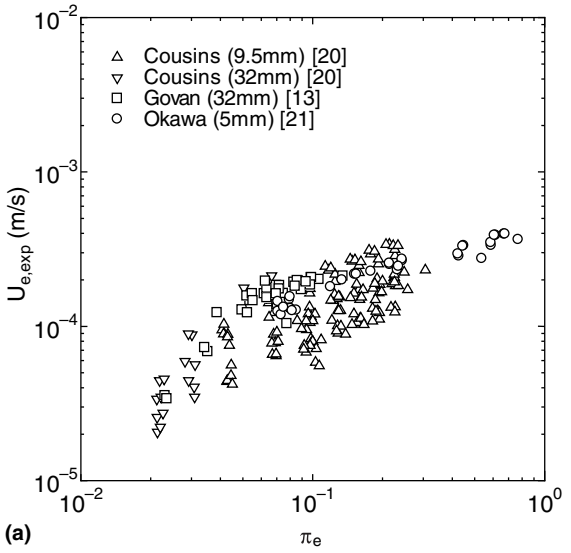

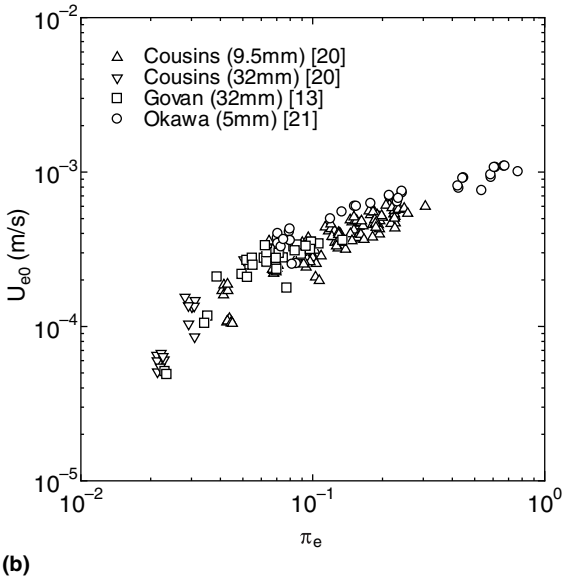

Fig. 9. Dependence of volumetric entrainment rate on π_e: (a) dependence of $U_{e,exp}$, (b) dependence of U_{e0}.

The following correlation by Ishii and Grolmes [28] is used to estimate J_{gc}:

$$\frac{\mu_l J_{gc}}{\sigma}\sqrt{\frac{\rho_g}{\rho_l}} = J^*_{gc} \tag{19}$$

where

$$J^*_{gc} = 1.5 Re_f^{-1/2} \quad \text{for } Re_f < 160 \tag{20}$$

$$J^*_{gc} = \min(11.78 N_\mu^{0.8}, 1.35) Re_f^{-1/3} \quad \text{for } 160 > Re_f < 1635 \tag{21}$$

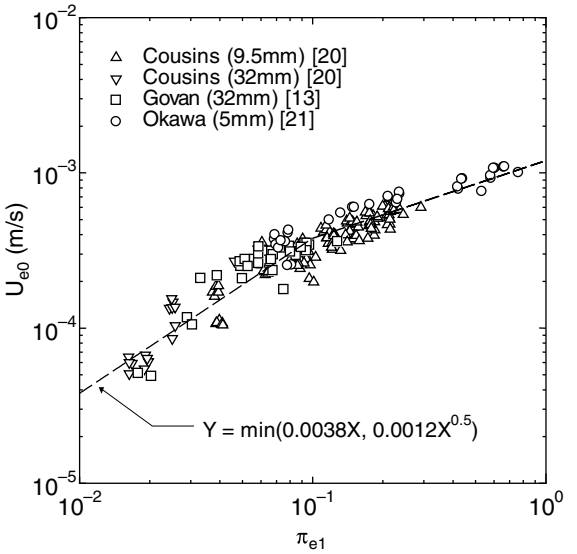

Fig. 10. Dependence of volumetric entrainment rate on π_{e1}.

$$J^*_{gc} = \min(N_\mu^{0.8}, 0.1146) \quad \text{for } Re_f > 1635 \tag{22}$$

$$N_\mu = \frac{\mu_l}{\sqrt{\rho_l \sigma}}\left(\frac{g\Delta\rho}{\sigma}\right)^{1/4} \tag{23}$$

The values of U_{e0} are plotted against π_{e1} in Fig. 10. Although the results are almost identical to those shown in Fig. 9(b), the parameter π_{e1} might be advantageous to introduce the inception criteria of droplet entrainment in the model. For the experimental data of air–water annular flow tested here, the following empirical correlation gives a reasonable fit:

$$U_{e0} = \min(k_{e1}\pi_{e1}, k_{e2}\pi_{e1}^{0.5}) \tag{24}$$

where the recommended values for k_{e1} and k_{e2} are 3.8×10^{-3} m/s and 1.2×10^{-3} m/s, respectively, as indicated with the dashed line in Fig. 10.

4. Validity of proposed correlations in wider experimental ranges

4.1. Deposition rate

The correlation for k_d developed in this study is summarized as follows. At low droplet concentration, k_d is evaluated by Eq. (11), that was originally developed by McCoy and Hanratty for long relaxation time particles [15]. At high droplet concentration, k_d is evaluated by Eq. (9). The boundary of C^* for the low and high droplet concentrations may be around 0.15. Thus, Eq. (11) is used if C^* is less than 0.1 while Eq. (9) if C^* is greater than 0.2. The interval between 0.1 and 0.2 is used for the smooth transition between the two correlations. In

the double film extraction experiments, k_d might be underestimated because of the influence of z^*. Hence, the experimental data of k_d should be transformed to k_{d0} through $k_{d0} = k_d f_z$. The correction function f_z is given by Eqs. (12) and (8) at low and high droplet concentrations, respectively. The deposition mass transfer coefficients $k_{d,cal}$ that are calculated for the experimental data listed in Table 1 are compared with the corrected experimental data $k_{d,exp}$ in Fig. 11. The agreement is fairly good as expected since this figure is a rearrangement of Figs. 5 and 8.

An important application of the present model is the use in the film flow analysis to predict the onset of dry-out in water saturated flow boiling. In view of this, the validity is tested against the experimental data for steam–water annular flow. Since the direct measurement of deposition rate in steam–water annular flow is scarce

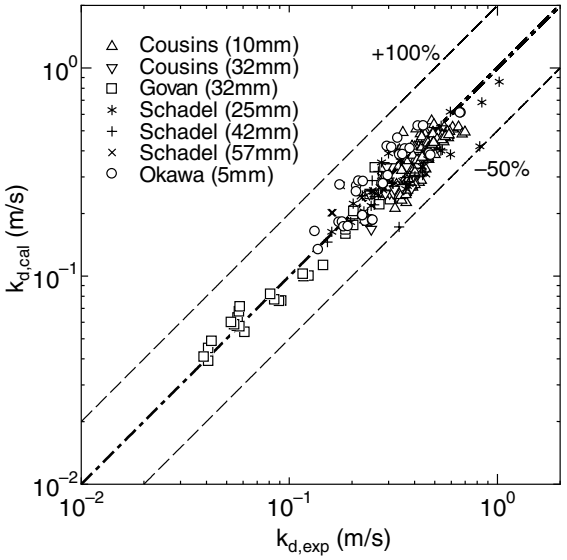

Fig. 11. Comparative representations of measured and predicted deposition mass transfer coefficients for air–water annular flows.

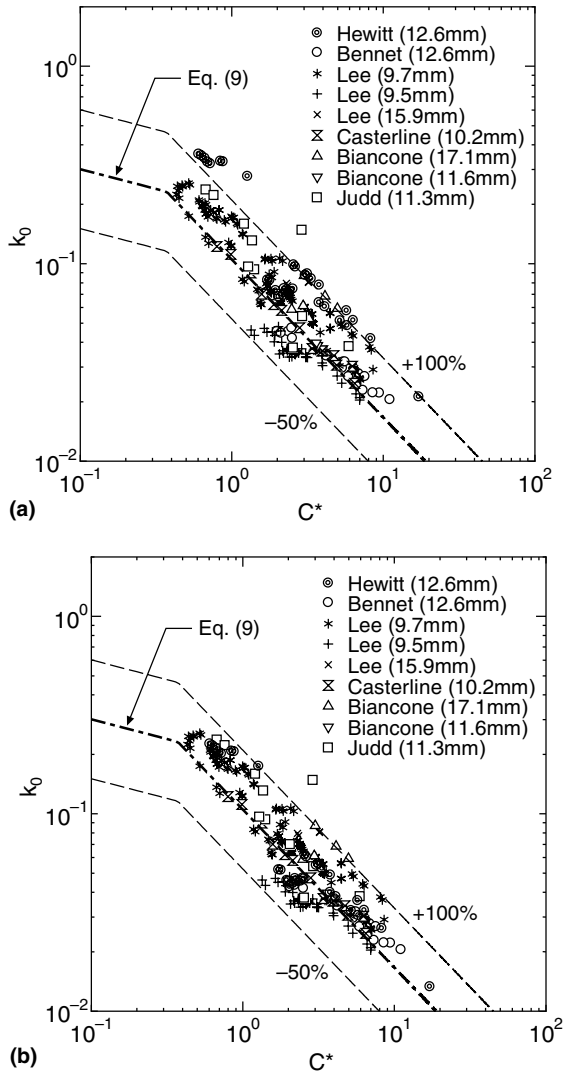

Fig. 12. Comparisons of the proposed deposition correlation with high-pressure steam–water data: (a) influence of deposition length is corrected, (b) influence of deposition length is not corrected.

Table 2
Experimental data of deposition rate for high-pressure steam–water annular flow

References	Measurement technique	D (mm)	z_d/D	N	ε_{1e}	ε_{2e}
Hewitt et al. [29]	Thermal method	12.6	12	31	−0.12	0.28
Bennet et al. [30]	Non-uniform heating	12.6	–	19	−0.04	0.17
Lee and Obertelli [31]	Non-uniform heating	9.7	–	134	−0.21	0.25
Lee [32]	Non-uniform heating	9.5	–	39	0.36	0.41
Lee [33]	Non-uniform heating	15.9	–	4	−0.40	0.41
Casterline and Matzner [34]	Non-uniform heating	10.2	–	14	−0.04	0.07
Biancone et al. [35]	Non-uniform heating	11.6	–	2	−0.05	0.05
Biancone et al. [35]	Non-uniform heating	17.1	–	6	−0.36	0.39
Judd et al. [36]	Non-uniform heating	11.3	–	11	−0.26	0.36

[29], the critical heat flux data in non-uniformly heated tubes [30–36] are also used to deduce the deposition rate of droplets. The experimental databases that are used to deduce the deposition mass transfer coefficient in steam–water annular flow are listed in Table 2. If the heat flux profile is axially non-uniform as in the case of chopped-cosine distribution, the onset of critical heat flux condition often occurs upstream of the exit of heated section. Since the film flowrate decreases upstream of the dryout point and then increases downstream, the spatial gradient of film flowrate is considered zero at the dryout point. Since the film flowrate is zero or very small at the dryout point, the entrainment rate may be neglected and the following mass balance equation holds [30]:

$$m_{\mathrm{d}} = \frac{q_{\mathrm{chf}}}{h_{\mathrm{gl}}} \tag{25}$$

where q_{chf} is the local heat flux at the dryout point and h_{gl} is the latent heat of vaporization. The deposition rate is consequently to be estimated from the critical heat flux data if the dryout point is known. To specify the burnout point for non-uniform axial heat flux profile, the local condition hypothesis is used (see Ref. [37] for the details of this method). The data in which the vapor quality at the burnout point is lower than that for the slug-annular transition are excluded in the following examinations since the mechanism of burnout is considered different from liquid film dryout. The vapor quality at the transition to annular flow was estimated from the correlation by Wallis [27]. Supposing that the length of non-entrainment section around the dryout point is sufficiently short, the deposition length is set at zero for the data that are deduced from the critical heat flux data for axially non-uniform heating. In all the steam–water data listed in Table 2, the dimensionless droplet concentration C^* is greater than 0.2. Hence, the correlation for the high droplet concentration Eq. (9) should be selected for the present steam–water data. For this reason, the experimental data of k_0 are plotted against C^* and compared with the correlation in Fig. 12(a). Despite the difficulty in the determination of dryout point, the correlation developed from the air–water data predicts the data for steam–water experiments fairly well. The notable deviations from the correlating line are found for the data by Hewitt et al. [29] that were measured with the thermal method. The deposition length adopted in this experiment was 12 tube diameters. Since the functional form of z^* shown in Eq. (8) was derived empirically using air–water data, some modification might be needed in high-pressure steam–water flow. It might be interesting to note that satisfactory agreements are achieved for the data by Hewitt et al. [29] if the influence of deposition length is not accounted as indicated in Fig. 12(b).

4.2. Entrainment rate

The proposed model for the entrainment rate Eq. (24) was developed from the experimental data of deposition rate in equilibrium air–water annular flow. The measurement of deposition rate in the equilibrium state was conducted extensively using air and water as test fluids but the experimental data for other fluids are scarce. Thus, the validity of the proposed model to steam–water annular flow is tested against the available experimental data of entrainment fraction. The experimental databases compiled for this purpose are listed in Table 3 [8,20,21,38–46]. In the quasi-equilibrium state, m_{d} may be balanced with the entrainment rate m_{e} since the flowrates of liquid film and droplets are almost constant

Table 3
Sources of entrainment fraction data

References	Fluids	D (mm)	N	ε_{1e}	ε_{2e}
Cousins and Denton [38]	Air–water	9.5	33	0.40	0.63
Cousins and Hewitt [20]	Air–water	9.5	571	0.47	0.59
Cousins and Hewitt [20]	Air–water	31.8	24	−0.13	0.18
Okawa et al. [21]	Air–water	5.0	173	−0.16	0.32
Whalley and Hewitt [39]	Air–water	31.8	137	−0.08	0.45
Owen et al. [40]	Air–water	31.8	49	−0.07	0.28
Asali [41]	Air–water	22.9	24	−0.28	0.36
Asali [41]	Air–water	42.0	28	−0.24	0.39
Schadel et al. [8]	Air–water	25.4	24	0.33	0.53
Schadel et al. [8]	Air–water	42.0	17	0.02	0.38
Schadel et al. [8]	Air–water	57.1	16	0.23	0.63
Hewitt and Pulling [42]	Steam–water	9.30	63	−0.13	0.27
Würtz [43]	Steam–water	10.0	71	0.08	0.55
Würtz [43]	Steam–water	20.0	21	0.24	0.39
Keeys et al. [44]	Steam–water	12.7	21	0.07	0.12
Nigmatulin et al. [45]	Steam–water	13.3	48	0.18	0.63
Singh et al. [46]	Steam–water	12.5	27	0.19	0.76

along the channel. Hence, the assumptions of thin liquid film and small relative velocity between the droplets and gas phase lead to

$$m_e \cong m_d = k_d C_{eq} \cong k_d \frac{E_{eq}\rho_l J_l}{J_g} \tag{26}$$

where C_{eq} and E_{eq} are the droplet concentration and entrainment fraction in the equilibrium state, respectively. From Eq. (26), U_e is expressed in terms of E_{eq} by

$$U_e = \frac{k_d E_{eq} J_l}{J_g} \tag{27}$$

The above equation indicates that the correlation for k_d is necessary to estimate the entrainment rate from E_{eq}; the correlation for k_d developed in this work is used to calculate U_e. The values of U_e calculated for air–water and steam–water experiments are plotted against π_{e1} in Fig. 13(a) and (b), respectively. In the figures, the data are eliminated if the distance from the gas–liquid mixing section is shorter than z_{eq} that is calculated from Eq. (13); also, the data are not plotted if E_{eq} is smaller than 0.05 since the small measurement error in the extracted film flowrate may lead to significant error in the droplet flowrate when E_{eq} is small. It is confirmed from Fig. 13(a) that the proposed correlation Eq. (24), that was developed from the experimental data of deposition rate, agrees well with the entrainment rates deduced from the experimental data of equilibrium entrainment fraction in air–water annular flow. However, the scattering is more prominent in Fig. 13(a) than in Fig. 10. This result would be attributed to the error in predicting k_d. For instance, the experimental data for 9.5 mm tube by Cousins and Hewitt [20] are overestimated particularly at large π_{e1} in Fig. 13(a). The present correlation for k_d has the tendency to underestimate the data by Cousins et al. at high droplet concentration as shown in Fig. 5. Eq. (27) indicates that the underestimation in k_d leads to the overestimation in U_e. The improvement of the correlation for the deposition mass transfer coefficient is hence considered essential to achieve better agreements in Fig. 13(a). Though the range of tube diameter in the databases that were used to develop the entrainment rate correlation is 5.0–31.8 mm, Fig. 13(a) may indicate that the same correlation is applicable to larger diameter tubes (see also the mean fractional error ε_{1e} and the standard deviation ε_{2e} in Table 3). Applicability of the same correlation to the experiment data of steam–water annular flow is tested in Fig. 13(b). Though a small number of data deviate from the correlating line significantly, most data are predicted with the present correlation fairly well. This may indicate that π_{e1} is an appropriate scaling parameter to characterize the rate of droplet entrainment. It is however found that Eq. (24) overestimates the data when π_{e1} is larger than unity. When Eq. (24) was derived from the experimental data of deposition rate in Fig. 10, no data were available in this large π_{e1} range. Also, Fig. 13(b) suggests that the influence of π_{e1} on U_e becomes less significant in this condition. Thus, the following modification of Eq. (24) provides better agreements at large π_{e1}:

$$U_e = \min(k_{e1}\pi_{e1}, k_{e2}\pi_{e1}^{0.5}, k_{e3}) \tag{28}$$

where the recommended value for k_{e3} is 1.2×10^{-3} m/s.

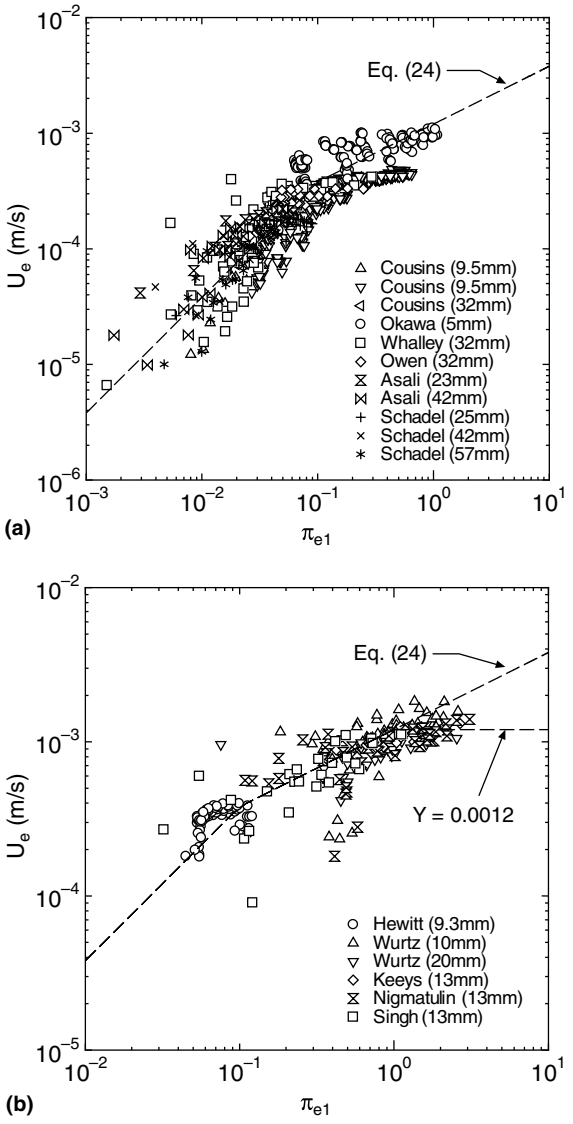

Fig. 13. Entrainment rate of droplets calculated from equilibrium entrainment fraction: (a) comparisons with air–water data, (b) comparisons with steam–water data.

5. Conclusions

The correlations for the deposition rate and entrainment rate of droplets in vertical upward annular flow

were developed from simple models and available experimental data. The main conclusions of this work are summarized as follows:

(1) It was found that the deposition mass transfer coefficient increases with the increase in volumetric flux of gas phase at low droplet concentration while decreases with the increase in droplet concentration at high droplet concentration. Thus, in the development of correlation for the deposition mass transfer coefficient, the volumetric flux of gas phase and the droplet concentration in gas core flow were used as a parameter of primary importance in low and high droplet concentrations, respectively. The simple correction functions for the deposition length in double film extraction experiments were important to achieve satisfactory agreements with the experimental data.
(2) It was confirmed that the dimensionless number denoting the ratio of interfacial shear force to surface tension force acting on the surface of liquid film is an appropriate scaling parameter to correlate the entrainment rate in annular two-phase flow.
(3) The present correlations for the deposition and entrainment rates were derived from available experimental data for air–water annular two-phase flows. The predicted results however agreed fairly well with the experimental data for high-pressure steam–water flows.

Acknowledgment

This work was funded by the Institute of Applied Energy (IAE), and Ministry of Economy, Trade and Industry (METI).

References

[1] K. Matsuura, A numerical study on droplet behavior in dispersed and annular-dispersed flows, Ph.D. thesis, Kyoto University, 2001 (in Japanese).
[2] L.G. Alexander, C.L. Colden, Droplet transfer from suspending air to duct walls, Ind. Eng. Chem. 43 (1951) 1325–1331.
[3] I.I. Paleev, B.S. Filippovich, Phenomena of liquid transfer in two-phase dispersed annular flow, Int. J. Heat Mass Transfer 9 (1966) 1089–1093.
[4] M. Yanai, A study on boiling heat transfer in a flow channel, Ph.D. thesis, Kyoto University, 1971 (in Japanese).
[5] S. Namie, T. Ueda, Droplet transfer in two-phase annular mist flow (part 1, experiment of droplet transfer rate and distributions of droplet concentration and velocity), Bull. JSME 15 (1972) 1568–1580.
[6] S. Namie, T. Ueda, Droplet transfer in two-phase annular mist flow (part 2, prediction of droplet transfer rate), Bull. JSME 16 (1973) 752.
[7] P. Andreussi, Droplet transfer in two-phase annular flow, Int. J. Multiphase Flow 9 (6) (1983) 697–713.
[8] S.A. Schadel, G.W. Leman, J.L. Binder, T.J. Hanratty, Rates of atomization and deposition in vertical annular flow, Int. J. Multiphase Flow 16 (1990) 363–374.
[9] K. Goldmann, G.H. Firstenber, C. Lombardi, Burnout in turbulent flow (a droplet diffusion model), Trans. ASME, J. Heat Transfer 83 (1961) 158–162.
[10] P.B. Whalley, G.F. Hewitt, The correlation of liquid entrainment fraction and entrainment rate in annular two-phase flow, AERE-R9187, 1978.
[11] T. Saito, E.D. Hughes, M.W. Carbon, Multi-fluid modeling of annular two-phase flow, Nucl. Eng. Des. 50 (1978) 225–271.
[12] S. Sugawara, Droplet deposition and entrainment modeling based on the three-fluid model, Nucl. Eng. Des. 122 (1990) 67–84.
[13] A.H. Govan, G.F. Hewitt, D.G. Owen, T.R. Bott, An improved CHF modelling code, in: Proceedings of the second UK National Heat Transfer Conference, 1988, pp. 33–48.
[14] T. Okawa, T. Kitahara, K. Yoshida, T. Matsumoto, I. Kataoka, New entrainment rate correlation in annular two-phase flow applicable to wide range of flow condition, Int. J. Heat Mass Transfer 45 (2002) 87–98.
[15] D.D. McCoy, T.J. Hanratty, Rate of deposition of droplets in annular two-phase flow, Int. J. Multiphase Flow 3 (1977) 319–331.
[16] J. Würtz, An experimental and theoretical investigation of annular steam–water flow in tube and annuli at 30 to 90 bar, Riso Report No. 372, 1978.
[17] I. Kataoka, M. Ishii, A. Nakayama, Entrainment and deposition rates of droplets in annular two-phase flow, Int. J. Heat Mass Transfer 43 (2000) 1573–1589.
[18] L. Pan, T.J. Hanratty, Correlation of entrainment for annular flow in vertical pipes, Int. J. Multiphase Flow 28 (2002) 363–384.
[19] T. Okawa, T. Kitahara, K. Yoshida, T. Matsumoto, I. Kataoka, A simple correlation of droplet entrainment rate in annular-dispersed two-phase flows, in: Proceedings of 4th International Conference on Multiphase Flow, 2001, Paper No. 396.
[20] L.B. Cousins, G.F. Hewitt, Liquid phase mass transfer in annular two-phase flow: droplet deposition and liquid entrainment, AERE-R5657, 1968.
[21] T. Okawa, A. Kotani, I. Kataoka, Experiments for liquid phase mass transfer in annular flow for a small vertical tube, Int. J Heat Mass Transfer 48 (2005) 585–598.
[22] G.F. Hewitt, Liquid-phase mass transfer rate in annular flow, in: G. Hetsroni (Ed.), Handbook of Multiphase Systems, McGraw-Hill, New York, 1982, Section 10.2.2.4.
[23] B.J. Azzopardi, Drops in annular two-phase flow, Int. J. Multiphase Flow 23 (1998) 1–53.
[24] P. Andreussi, B.J. Azzopardi, Droplet deposition and interchange in annular two-phase flow, Int. J. Multiphase Flow 9 (1983) 681–695.

[25] M.A. Lopez de Bertodano, A. Assad, S.G. Beus, Experiments for entrainment rate of droplets in the annular regime, Int. J. Multiphase Flow 27 (2001) 685–699.
[26] M. Ishii, K. Mishima, Droplet entrainment correlation in annular two-phase flow, Int. J. Heat Mass Transfer 32 (1989) 1835–1846.
[27] G.B. Wallis, One-Dimensional Two-Phase Flow, McGraw-Hill, New York, 1969.
[28] M. Ishii, M.A. Grolmes, Inception criteria for droplet entrainment in two-phase concurrent film flow, AIChE J. 21 (1975) 308–318.
[29] G.F. Hewitt, H.A. Kearsey, R.K.F. Keeys, Determination of rate of deposition of droplets in a heated tube with steam–water flow at 1000 psia, AERE-R6118, 1969.
[30] A.W. Bennett, G.F. Hewitt, H.A. Kearsey, R.F.K. Keeys, D.J. Pulling, Studies of burnout in boiling heat transfer to water in round tubes with non-uniform heating, AERE-R5076, 1966.
[31] D.H. Lee, J.D. Obertelli, An experimental investigation of forced convection burnout in high pressure water (Part 2, Preliminary results for round tubes with non-uniform axial heat flux distribution), AEEW-R309, 1963.
[32] D.H. Lee, An experimental investigation of forced convection burnout in high pressure water (Part 3, Long tubes with uniform and non-uniform axial heating), AEEW-R355, 1965.
[33] D.H. Lee, An experimental investigation of forced convection burnout in high pressure water (Part 4, Large diameter tubes at about 1600 psi), AEEW-R479, 1966.
[34] J.E. Casterline, B. Matzner, Burnout in long vertical tubes with uniform and cosine heating using water at 1000 psia, Columbia University, TID-21031, 1964.
[35] F. Biancone, A. Campanile, G. Galimi, M. Goffi, Forced convection burnout and hydrodynamic instability experiments for water at high pressure (Part 1, Presentation of data for round tubes with uniform and non-uniform power distribution), EUR2490e, 1965.
[36] D.F. Judd, R.H. Wilson, C.P. Welch, R.A. Lee, J.W. Ackerman, Non-uniform heat generation experimental program (Quarterly progress report No. 7), BAW-3238-7, 1965.
[37] J.G. Collier, Convective Boiling and Condensation, second ed., McGraw-Hill, New York, 1972.
[38] L.B. Cousins, W.H. Denton, G.F. Hewitt, Liquid mass transfer in annular two-phase flow, in: Proceedings of Symposium on Two-Phase Flow, Exeter, Paper C4, 1965.
[39] P.B. Whalley, G.F. Hewitt, P. Hutchinson, Experimental wave and entrainment measurements in vertical annular two-phase flow, AERE-R7521, 1973.
[40] D.G. Owen, G.F. Hewitt, T.R. Bott, Equilibrium annular flows at high mass fluxes; data and interpretation, PCH PhysicoChem. Hydrodyn. 6 (1985) 115–131.
[41] J.C. Asali, Entrainment in vertical gas–liquid annular flows, Ph.D. thesis, University of Illinois, 1983.
[42] G.F. Hewitt, D.J. Pulling, Liquid entrainment in adiabatic steam–water flow, AERE-R5374, 1969.
[43] J. Würtz, An experimental and theoretical investigation of annular steam–water flow in tube and annuli at 30 to 90 bar, Riso Report, No. 372, 1978.
[44] R.F.K. Keeys, J.C. Ralph, D.N. Roberts, Liquid entrainment in adiabatic steam–water flow at 500 and 1000 psia, AERE-R6293, 1970.
[45] B.I. Nigmatulin, V.I. Malyshenko, Y.Z. Shugaev, Investigation of liquid distribution between the core and the film in annular dispersed flow of steam/water mixture, Teploenergetika 23 (1976) 66–68.
[46] K. Singh, C.C. St. Pierre, W.A. Cargo, E.O. Moeck, Liquid film flowrates in two-phase flow of steam and water at 1000 psia, AIChE J. 15 (1969) 51–56.